Theor Chem Acc (2001) 106:22–27
DOI 10.1007/s002140100259

Theoretical
Chemistry Accounts

Regular article

Prediction of DNA far-IR absorption spectra based on normal mode analysis

**Maria Bykhovskaia[1], Boris Gelmont[2], Tatiana Globus[2], Dwight L. Woolard[3], Alan C. Samuels[4]
Tap Ha Duong[5], Krystyna Zakrzewska[5]**

[1] Department of Molecular Physiology and Biological Physics, University of Virginia, Charlottesville, VA 22906-0011, USA
[2] Department of Electrical Engineering, University of Virginia, Charlottesville, VA 22906-0011, USA
[3] U.S. Army Research Office, Research Triangle Park, NC 27709, USA
[4] Edgewood Chemical Biological Center, Proving Ground, MD 21010, USA
[5] Laboratoire de Biochimie Théorique, Institut de Biologie Physico-Chimique, 13 rue Pierre et Marie Curie, 75005 Paris, France

Received: 20 June 2000 / Accepted: 5 January 2001/ Published online: 3 May 2001

Abstract. We present a computational method which couples normal mode analysis in internal coordinates of a molecule with very far IR spectroscopy. The analytical expression for the dependence of IR absorption on frequency incorporates frequencies and optical activities of each normal mode. In order to predict far-IR spectra of a molecule we evaluate the optical activity of each normal mode. This optical activity is determined by the vibration amplitude of the dipole moment produced by a normal mode. We calculated normal modes of DNA double-helical fragments $(dA)_{12} \cdot (dT)_{12}$ and $(dA\text{-}dT)_6 \cdot (dA\text{-}dT)_6$ and evaluated their optical activities. These were found to be very sensitive to the DNA base-pair sequence. The positions of the resonance peaks in the calculated absorption spectrum of $(dA)_{12} \cdot (dT)_{12}$ are in a good agreement with those obtained by Fourier transform IR spectroscopy (Powell JW et al. 1987 *Phys Rev A* 35: 3929–3939).

Key words: Oligonucleotides – B-helix – Infrared spectroscopy – Dipole moment – Oscillator strength

1 Introduction

DNA low-frequency internal vibrations play an important role in many biological processes, such as transcription, viral infection and molecular recognition [1]. Well-known computational methods for studying the dynamics of biopolymers are molecular dynamics (reviewed in Ref. [2]) and normal mode analysis [3, 4, 5, 6, 7]. Normal mode analysis allows calculations of molecular vibrations around an energy minimum by making a harmonic approximation to the local energy hypersurface. The advantages of normal mode analysis for studying the dynamics of macromolecules are that it is a relatively rapid computational technique and that the calculated vibrational frequencies can be compared with resonance frequencies found by spectroscopic methods, either Raman [8] or absorption.

DNA IR absorption measurements [9, 10] coupled with lattice dynamic analysis [11] demonstrated that DNA low-frequency vibrations produce characteristic absorption bands in the far-IR region (between 40 and 300 cm^{-1}) which are sensitive both to DNA composition and to environment [10]. Our own IR absorption measurements of salmon DNA [12] revealed that in the long-wave spectrum region (from 2 to 250 cm^{-1}) the resonance peaks have a very high density. These results could be predicted from the computational studies of DNA normal modes [7], where the density of frequencies corresponding to rotational modes was found to be about 1 per reciprocal centimeter. Since vibrations of DNA covalent bonds have frequencies over 750 cm^{-1} [13], it is not necessary to consider vibrations of covalent bonds in order to predict the very far IR absorption spectra; therefore, normal mode analysis in internal coordinates of a molecule (torsion and bond angles) is the most appropriate method for the theoretical study of low-frequency resonance modes of nucleic acids [6, 7].

However, for the accurate comparison of theory and experiment it is important to account for differences in absorption by different modes. We present here a method for calculation of far-IR absorption spectra of a molecule based on the normal mode analysis in internal

Correspondence to: M. Bykhovskaia
Contribution to the Symposium Proceedings of Computational Biophysics 2000

molecular coordinates. We performed the calculations of the absorption spectra for two DNA fragments consisting of 12 base pairs, $(dA)_{12}\cdot(dT)_{12}$ and $(dA\text{-}dT)_6\cdot(dA\text{-}dT)_6$, and compared the predicted spectra with the results of Fourier transform IR measurements [10].

2 Methods

2.1 Relationship between normal modes and absorption spectra

The dependence of the permittivity, ε, on the radiation frequency, ω, can be described by the Kramers–Heisenberg dielectric function:

$$\varepsilon(\omega) = \varepsilon_\infty + 4\pi N \sum_k S_k/3\left(\omega_k^2 - \omega^2 - i2\pi\gamma_k\omega\right) \ , \tag{1}$$

where the k denotes normal modes, ω_k are vibrational frequencies, S_k are oscillator strengths, γ_k are oscillators dissipations and N is the number of molecules.

The absorption coefficient, α, is proportional to the imaginary part of the permittivity,

$$\alpha = (\omega/nc)\mathrm{Im}(\varepsilon); \tag{2}$$

hence, its dependence on frequency, ν ($\nu = \omega/2\pi$), is determined by

$$\alpha(\nu)\tilde{\nu}^2 \sum_k S_k\gamma_k/\left[\left(\nu_k^2 - \nu^2\right)^2 + (\gamma_k\nu)^2\right] \ . \tag{3}$$

Normal mode analysis enables calculations of eigenfrequencies, ν_k. Oscillator strengths, S_k, can be found from calculations of the vibrational trajectory along each normal mode (see later). Oscillator dissipations, γ_k, cannot be found from a harmonic approximation of the potential energy and, hence, remain to be determined from the comparison of theory and experiment. In the first approximation, however, the decay can be considered frequency-independent. In this simplified form the absorption depends on the frequency as

$$\alpha(\nu)\tilde{\nu}^2\gamma \sum_k S_k/\left[\left(\nu_k^2 - \nu^2\right)^2 + (\gamma\nu)^2\right] \ . \tag{4}$$

2.2 Energy minimization and normal mode analysis

Standard B-helical conformations were created using the program package JUMNA [14, 15, 16, 17]. The conformational energy was calculated as the sum of the energy of van der Waals and electrostatic interactions, torsion rotation potentials, harmonic potentials of bond-angle deformations, and the energy of hydrogen bond deformations using the FLEX force field [18]. The energy was minimized in the space of the internal coordinates of a molecule (torsion and bond angles) using the software package LIGAND [19].

The normal modes (eigenfrequencies, **W**, and eigenvectors, **A**) were calculated in the space of internal variables as solutions of the equation

$$\mathbf{HAW} = \mathbf{FA} \ , \tag{5}$$

where **W** is a diagonal matrix with elements ω_k^2 (vibrational frequencies); **F** is a matrix of second derivatives of potential energy and **H** is a matrix of second derivatives of kinetic energy. The normal modes (eigenvectors, **A**, and eigenfrequencies, **W**) were calculated as described in Ref. [7] using the program LIGAND.

2.3 Oscillator strengths

Each normal vibration produces fluctuations of the dipole moment of a molecule. The oscillator strength, S_k, corresponding to the kth normal mode can be expressed as the square of the normalized amplitude, **p**, of the dipole moment deviation [20]:

$$S_k = (\mathbf{p}^k)^2 \ . \tag{6}$$

The normalized dipole moment, **p**, can be expressed as

$$\mathbf{p} = \sum_i e_i\mathbf{a}_i/\sqrt{m_i} \ , \tag{7}$$

where the index i denotes atoms, e_i are partial atomic charges, m_i are atomic masses, and $\mathbf{a}_i$ are eigenvectors in atomic Cartesian coordinates (atomic displacements) normalized in such a way that

$$\sum_i (\mathbf{a}_i)^2 = 1 \ . \tag{8}$$

Equation (7) was obtained [20] under the classical mechanical approximation ($h\nu \ll k_\mathrm{B}T$); however, we show in the Appendix that Eqs. (4) and (7) are also applicable in the ultraquantum approximation ($h\nu \gg k_\mathrm{B}T$).

Since the normal mode analysis was performed in internal coordinates of a molecule, atomic displacements, $\mathbf{a}_i$, are not readily available from the matrix of eigenvectors, **A** (solution of Eq. 5), as it would be if eigenmodes were calculated in atomic Cartesian coordinates [8]. Therefore, for each mode we created structures within the limits of thermal energy [7] and calculated deviations of the molecular dipole moment from the structure in the energy minimum.

2.4 Summary of the calculation protocol

The procedure consists of

1. Initial optimization of the B-helix using the program JUMNA.
2. Energy minimization and calculation of normal modes (eigenfrequencies, ω_k, and eigenvectors, $\mathbf{A}_k$) using the program LIGAND.
3. Calculation of the three-dimensional structures along normal mode vectors [7].
4. Calculation of oscillator strengths. The variable dipole moment of a molecule, **P**, is calculated as

$$\mathbf{P} = \sum e_i\mathbf{r}_i \ , \tag{9}$$

where the index i denotes atoms and the vector $\mathbf{r}_i$ is a displacement of the ith atom from equilibrium. The oscillator strengths, S_k, are calculated as

$$S_k = (\mathbf{P}^k)^2_{\max}/\sum m_i(\mathbf{r}_i)^2_{\max} \ , \tag{10}$$

where $\mathbf{P}^k$ is produced by the kth vibration.
5. Calculation of absorption spectra, $\alpha(\nu)$ (Eq. 4). A realistic estimation of γ obtained from the measurements of $(dA)_{12}\cdot(dT)_{12}$ absorption spectra is from 2 to 7 cm^{-1} [10].

3 Results

The oligonucleotides $(dA)_{12}\cdot(dT)_{12}$ and $(dA\text{-}dT)_6\cdot(dA\text{-}dT)_6$ have 360 degrees of freedom in the space of the internal coordinates (torsion and bond angles). For each sequence, 360 normal modes were found. Their frequencies lie below 900 cm^{-1} (Fig. 1), so there is almost no overlap with vibrations of covalent bonds which have frequencies above 750 cm^{-1} [21]. The two oligonucleotides have similar mode densities in the region above 250 cm^{-1}, which essentially involve vibrations of valence angles [7]. It could be expected that the modes that reflect vibrations of torsion angles would be more sensitive to the conformation and flexibility of the helix. Indeed, the calculated density spectra of the two oligomers differ markedly in the region below 250 cm^{-1}. Specifically, $(dA\text{-}dT)_6\cdot(dA\text{-}dT)_6$ has very distinct peaks around 15 and 175 cm^{-1}, while homoplymer $(dA)_{12}\cdot(dT)_{12}$ has a broad spectrum with no pronounced peaks (Fig. 1). The earlier normal mode analysis of $(dA\text{-}dT)_6\cdot$

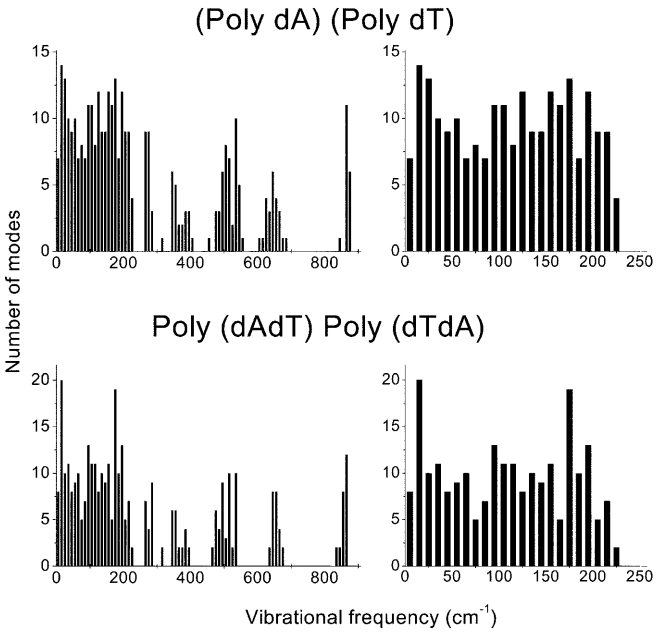

Fig. 1. Density of normal modes. The histograms on the *left* represent all the calculated modes. The scale is expanded (*right panels*) to show the low-frequency modes

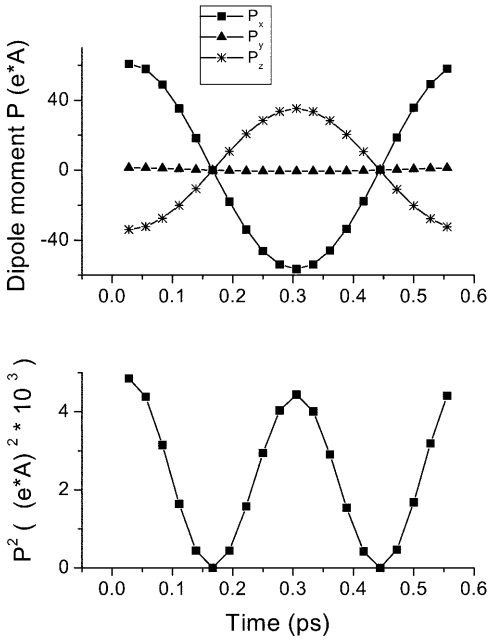

Fig. 2. Fluctuations of the dipole moment, $\mathbf{P}^k$, of $(dA\text{-}dT)_6{\cdot}(dA\text{-}dT)_6$ corresponding to a normal vibration with a frequency of 60.3 cm^{-1} at room temperature. The double helix is oriented along the *z*-axis. The amplitude of the $(\mathbf{P}^k)^2$ fluctuation (*bottom*) is used in Eq. (10)

$(dA\text{-}dT)_6$ performed with rigid valence angles [7] revealed only one peak at 15 cm^{-1}, which indicates that the second peak at 175 cm^{-1} essentially involves vibrations of valence angles.

For each resonance mode we examined deviations of the dipole moment, $\mathbf{P}^k$ (Eq. 9). The period of the dipole moment vibration for the strongest mode with the frequency near 60 cm^{-1} is shown in Fig. 2. We chose this mode as an example because both $(dA)_{12}{\cdot}(dT)_{12}$ and $(dA\text{-}dT)_6{\cdot}(dA\text{-}dT)_6$ demonstrate a strong resonance absorption at a frequency of 60 cm^{-1} [10]. This mode was previously assigned to vibrations along the helix axis (*z*); however, Fig. 2 demonstrates that the traverse component, P_x, has comparable amplitude.

The amplitude of $\mathbf{P}^2$ fluctuations determines the strength of each vibration (Eq. 10). We found that the normal modes of the two oligomers examined have strikingly different spectra of the oscillator strengths. For the molecule with homogeneous strands, $(dA)_{12}{\cdot}(dT)_{12}$, the oscillator strengths appeared to be very uniform, while heterogeneity in the strand composition introduced many-fold variance (Fig. 3). The two low-frequency modes of $(dA)_{12}{\cdot}(dT)_{12}$ (2.64 and 2.69 cm^{-1}) have strengths 3–4 times greater than the average strength for the other modes (Fig. 3). These two low-frequency vibrations have strong **P** components perpendicular to the helical axis and may reflect helical bending [7, 22]. The strongest modes of the heteropolymer (Fig. 3) also lie in the low-frequency range (mostly below 50 cm^{-1}). This result is not surprising, for the strongest modes reflect the relative motions of the strands, which in turn involve low-frequency torsion rotations.

We calculated the absorption spectra of the two molecules (Fig. 4) according to Eq. (4) using two reasonable approximations for the band width, γ, obtained experimentally (2 and 7 cm^{-1} [10]). The positions of the resonance peaks do not depend on the band width (Fig. 5), and in the longer-wavelength range (below 220 cm^{-1}) they are remarkably similar to those observed experimentally (Table 1).

Another similarity of the calculated and experimental spectra is the steep fall in the absorption intensities as the frequency exceeds 250 cm^{-1} for both sequences. This feature is caused by the decrease in the normal mode densities and is not related to their optical properties. Finally, $(dA\text{-}dT)_6{\cdot}(dT\text{-}dA)_6$ demonstrates higher absorption at lower frequencies (below 100 cm^{-1}) owing to the higher oscillator strengths of its lower-frequency modes, while $(dA)_{12}{\cdot}(dT)_{12}$ has a plateau between 20 and 200 cm^{-1}. This difference in the spectra has also been observed experimentally [10].

The calculated spectra have a strong resonance peak around 20 cm^{-1} for both sequences. While no experimental data on IR absorption is available in this frequency range, Raman scattering [23] clearly indicates resonance peaks around 20 cm^{-1} (16.2, 19.3 and 23.3 cm^{-1}).

4 Discussion

We presented a calculation of DNA IR active modes directly from the sequence and topology of the molecule. Unlike most of the other studies on DNA theoretical spectroscopy [11, 23, 24, 25, 26], we did not oversimplify the DNA structure and considered all possible interatomic interactions. To do that, we employed the methods of molecular mechanics and normal mode analysis, which enable rigorous calculations of biopolymer structure and dynamics (reviewed in Ref. 28). Thus,

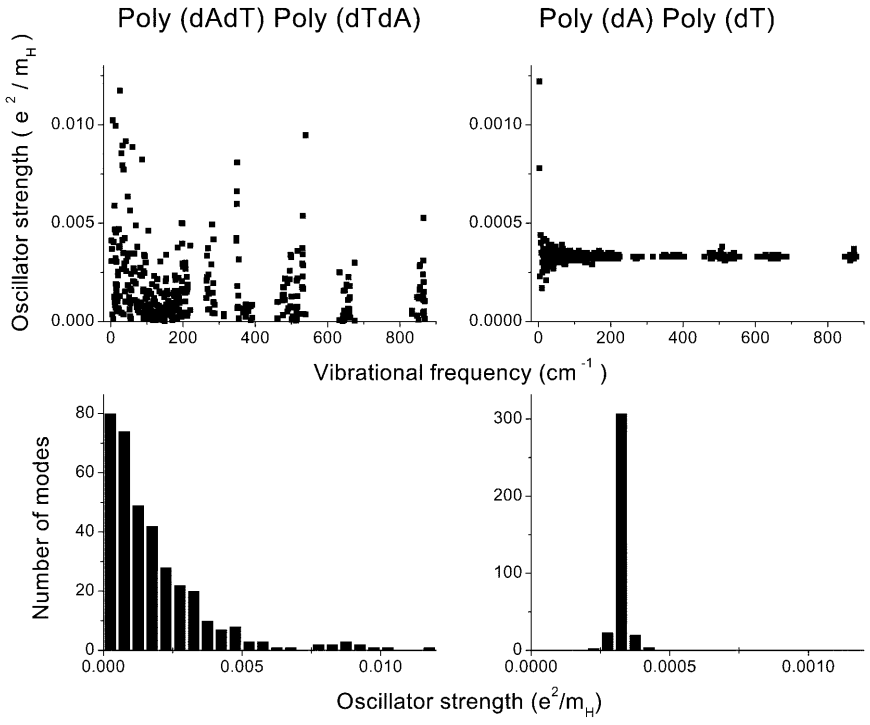

Fig. 3. Spectra of oscillator strengths

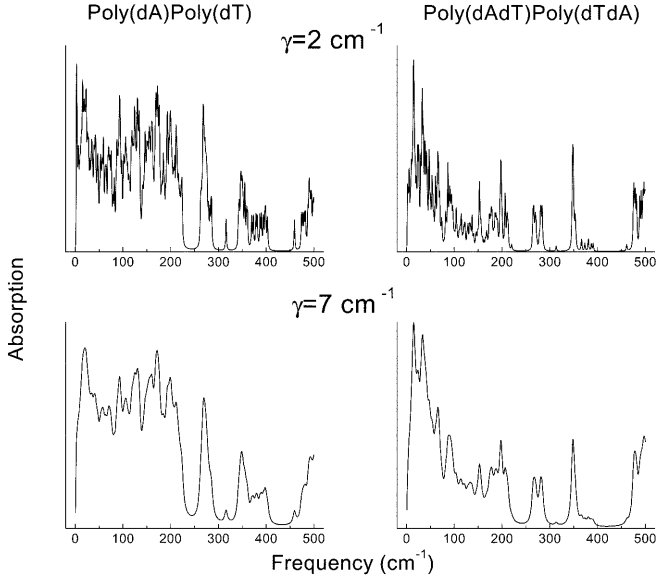

Fig. 4. Absorption spectra (arbitrary units) calculated for two values (2 and 7 cm^{-1}) of the band width, γ

Table 1. Resonance frequencies for $(dA)_{12}\cdot(dT)_{12}$. All *numbers* are in reciprocal centimeters

Calculations	Experiment [10]
20	Unknown
43	Unknown
57	62
71	80
94	95
106	106
131	136
160	–
172	170
199	–
211	214
–	238
270	–
348	–
400	–
459	–

our study presents a link between molecular modeling and the theoretical spectroscopy of DNA.

A resonance peak is often assigned to a certain type of vibration, which is assumed to have a strong optical activity [10, 28, 29, 30]. Our study shows that care should be taken with the straightforward assignments, for a resonance peak can be produced as well by an increased density of weak normal modes. This is by and large the case for the homopolymer $(dA)_{12}\cdot(dT)_{12}$, which mostly has vibrations perpendicular to the helical axis with uniform strengths. However, nonuniformity in the optical activity of the normal modes can essentially alternate the optical spectra for molecules with heterogeneous structure, as was observed for $(dA\text{-}dT)_6\cdot(dT\text{-}dA)_6$. Our analysis makes it possible to understand the physical nature of many spectral features. Thus, the decrease in the absorption intensities observed for frequencies above 250 cm^{-1} [9, 10, 12] is obviously due to the fact that most of the low-frequency vibrations involve torsion rotations and their frequencies lie below 250 cm^{-1}.

For an accurate calculation of optical spectra, the dependence of a resonance mode decay on its frequency is required. In our study, it was roughly approximated on the basis of experimental data [10]. However, the positions of the resonance peaks are not substantially

affected by this parameter, though in principle an increase in the band width can essentially diminish and even eliminate some of the peaks. The oscillator decay has a tendency to increase as its frequency increases. This is likely to be the reason why several peaks with frequencies above 250 cm^{-1} predicted by our calculations were not observed experimentally (Table 1).

In spite of many factors, such as variability of molecule length and interaction with salt and water molecules, the absorption peaks calculated in our study for $(dA)_{12}\cdot(dT)_{12}$ reproduced most of the peaks observed in Fourier transform IR spectroscopy [10]; thus, the analysis presented has considerable potential for the prediction of DNA optical properties.

Appendix

The interaction Hamiltonian with the electric field, **F**, is

$$V_F = (\mathbf{FP}) \ , \tag{A1}$$

where **P** is the deviation of the dipole moment of a molecule (see Methods). For the kth normal mode, the dipole moment has nonzero matrix elements for the transitions between neighboring quantum levels n_k and n_k+1:

$$\langle n_k|\mathbf{P}|n_k+1\rangle = \mathbf{p}^{(k)}\sqrt{\hbar(n_k+1)/(2\omega_k)} \ . \tag{A2}$$

The levels are populated in accordance with the Planck function:

$$N_k(\nu_k) = \left[\exp\left(\frac{h\nu_k}{k_B T}\right) - 1\right]^{-1} \ . \tag{A3}$$

According to Equation (A3), the population of excited levels will be negligible if $h\nu > k_B T$; therefore, the electric field will cause only transitions between the ground-state level with $n_k = 0$ and first excited level with $n_k = 1$. Hence, only the two lowest levels are essential for absorption, which enables us to use the equations for the density matrix, ρ, of a two-level system derived in Ref [31]. Off-diagonal matrix elements for the two-level system can be expressed as [31]

$$i\frac{\partial\rho_{01}^{(k)}}{\partial t} - \omega_k\rho_{01}^{(k)} + i\pi\gamma_k\rho_{01}^{(k)} = \frac{\left(\mathbf{Fp}^{(k)}\right)}{\sqrt{2\hbar\omega_k}}\left(\rho_{11}^{(k)} - \rho_{00}^{(k)}\right) \ , \tag{A4}$$

where γ is the reciprocal transverse relaxation time. The solution of this equation is

$$\rho_{01}^{(k)} = \frac{\left(\mathbf{Fp}^{(k)}\right)}{\sqrt{2\hbar\omega_k}}\frac{\rho_{11}^{(k)} - \rho_{00}^{(k)}}{\omega_k - \omega - i\pi\gamma_k} \ , \tag{A5}$$

where $\rho_{10}^{(k)}$ is a conjugate value. The average dipole moment can be found as

$$\langle\mathbf{P}(\omega)\rangle = \mathrm{Tr}(\rho\mathbf{P}) = \sum_k \frac{\rho_{00}^{(k)} - \rho_{11}^{(k)}}{2\omega_k}\left(\frac{1}{\omega_k - \omega - i\pi\gamma_k} + \frac{1}{\omega_k + \omega + i\pi\gamma_k}\right)\mathbf{p}^{(k)}\cdot\left(\mathbf{p}^{(k)}\mathbf{F}\right) \tag{A6}$$

Hence the susceptibility of each molecule is

$$\chi_{\alpha\beta}(\omega) = \sum_k \frac{p_\alpha^{(k)} p_\beta^{(k)}}{\omega_k^2 - (\omega + i\pi\gamma_k/2)^2}\left(\rho_{00}^{(k)} - \rho_{11}^{(k)}\right) \ . \tag{A7}$$

Considering that only the ground-state level is occupied ($\rho_{00} = 1$ and $\rho_{11} = 0$) and that $\gamma \ll \omega$, the permittivity at low temperatures ($h\nu_k > k_B T$) coincides with an equation (Eqs. 4, 6, see Methods) derived from the classical mechanical approach.

References

1. Sinden RR (1994) DNA structure and function. Academic, San Diego
2. McCammon JA, Harvey SC (1986) Dynamics of proteins and nucleic acids. Cambridge University Press, Cambridge
3. Noguti T, Go N (1982) Nature 226: 776–778
4. Brooks B, Karplus M (1983) Proc Natl Acad Sci USA 80: 6571–6575
5. Levitt M, Sander C, Stern PS (1985) J Mol Biol 181: 423–447
6. Lin D, Matsumoto A, Go N (1997) J Chem Phys 107: 3684–3690
7. Duong TH, Zakrzewska K (1997) J Comput Chem 18: 796–811
8. Melchers P, Knapp EW, Parak F, Cordone L, Cupane A, Leone M (1996) Biophys J 70: 2092–2099
9. Wittlin A, Genzel L, Kremer K, Haseler H, Poglitsch A, Rupprecht A (1986) Phys Rev A 34: 493–500
10. Powell JW, Edwards GS, Genzel L, Kremer F, Wittlin A, Kubasek W, Peticolas W (1987) Phys Rev A 35: 3929–3939
11. Young L, Prabhu VV, Prohofsky EW (1989) Phys Rev 39: 3173–3179
12. Globus TR, Woolard DL, Bykhovskaia M, Gelmont B, Hesler JL, Crowe TW, Samuels AC (1999) International Semiconductor Device Research Symposium (ISDRS), Proceedings. Charlottesville, Va
13. Tailandier E, Liquier L (1992) In: Lilley DMJ, Dahlberg JE (eds) Methods in enzymology, vol 1: DNA structure. Part A. Synthesis and physical analysis of DNA. Academic, New York, pp 307–335
14. Poncin M, Hartmann B, Lavery R (1992) J Mol Biol 226: 775–794
15. Lavery R (1988) In: Olson WK, Sarna RH, Sarna MH, Sandaralingam M (eds) Structure and expression, vol 3: DNA bending and curvature. Adenine, New York, pp 191–211
16. Lavery R Zakrzewska K, Sklenar H (1995) Comput Phys Commun 91: 135–142
17. Lavery R, Hartmann B (1994) Biophys Chem 60: 33–43
18. Lavery R, Sklenar H, Zakrzewska K, Pulman B (1986) J Biomol Struct Dyn 3: 989–998
19. Lavery R, Parker I, Kendrick J (1986) J Biomol Struct Dyn 4: 989–998
20. Born M, Huang K (1968) The dynamical theory of crystal lattices. Clarendon, Oxford
21. Parker FS (1983) Applications of infrared, Raman, and resonance Raman spectroscopy in biochemistry. Plenum, New York, pp 349–359
22. Eyster JM, Prohofski EW (1974) Biopolymers 13: 2527–2543
23. Lisy V, Miskovsky P, Brutovsky B, Chinsky L (1997) J Biomol Struct Dyn 14: 517–523
24. Feng Y, Prohofski EM (1990) Biophys J 57: 547–553
25. Saxena VK, Van Zandt LL, Schroll (1989) Phys Rev A 39: 1474–1481
26. Saxena VK, Van Zandt LL (1994) Biophys J 67: 2448–2453
27. Lafontaine I, Lavery R (1999) Curr Opin Struct Biol 9: 170–176

28. Beetz CP, Ascarelli G (1982) Biopolymers 21: 1569–1570
29. WN, Kohli M, Prohofski EW, Van Zandt (1981) Biopolymers 20: 833–852
30. Lindsay M, Powell JW, Prohofski EW, Devi-Prasad KV (1984) In: Clementi E, Corogngiu G, Sarma MH, Sarma RH (eds) Structure and dynamics of nucleic acids, proteins and membranes. Adenine, New York, pp 531–556
31. Gelmont B, Gorfinkel V, Luryi S (1996) Appl Phys Lett 68: 2171–2173